

# GBPI, a novel gastrointestinal- and brain-specific PP1-inhibitory protein, is activated by PKC and inactivated by PKA

Qing-Rong LIU\*, Ping-Wu ZHANG\*, Zhicheng LIN\*, Qi-Fu LI†, Amina S. WOODS‡, Juan TRONCOSO§ and George R. UHL\*<sup>1</sup>

\*Molecular Neurobiology Branch, National Institute on Drug Abuse–Intramural Research Program (NIDA–IRP), NIH, Department of Health and Human Services (DHSS), Box 5180, Baltimore, MD 21224, U.S.A., †Laboratory for Cell Biology and Tumor Cell Engineering, Xiamen University, Xiamen, Fujian 361005, People's Republic of China, ‡Chemistry and Drug Metabolism Section, National Institute on Drug Abuse–Intramural Research Program (NIDA–IRP), NIH, Department of Health and Human Services (DHSS), Box 5180, Baltimore, MD 21224, U.S.A., and §Department of Pathology (Neuropathology), Johns Hopkins School of Medicine, Baltimore, MD 21287, U.S.A.

The activities of PP1 (protein phosphatase 1), a principal cellular phosphatase that reverses serine/threonine protein phosphorylation, can be altered by inhibitors whose activities are themselves regulated by phosphorylation. We now describe a novel PKC (protein kinase C)-dependent PP1 inhibitor, namely GBPI (gut and brain phosphatase inhibitor). The shorter mRNA that encodes this protein, GBPI-1, is expressed in brain, stomach, small intestine, colon and kidney, whereas a longer GBPI-2 splice variant mRNA is found in testis. Human GBPI-1 mRNA encodes a 145-amino-acid, 16.5 kDa protein with pI 7.92. GBPI contains a consensus PP1-binding motif at residues 21–25 and consensus sites for phosphorylation by enzymes, including PKC, PKA (protein kinase A or cAMP-dependent protein kinase) and casein kinase II. Recombinant GBPI-1-fusion protein inhibits PP1 activity with  $IC_{50} = 3$  nM after phosphorylation by PKC. Phospho-GBPI can even enhance PP2A activity by > 50% at submicromolar concentrations. Non-phosphorylated GBPI-1 is inactive in both assays.

Each of the mutations in amino acids located in potential PP1-binding sequences, K21E + K22E and W25A, decrease the ability of GBPI-1 to inhibit PP1. Mutations in the potential PKC phosphoacceptor site T58E also dramatically decrease the ability of GBPI-1 to inhibit PP1. Interestingly, when PKC-phosphorylated GBPI-1 is further phosphorylated by PKA, it no longer inhibits PP1. Thus, GBPI-1 is well positioned to integrate PKC and PKA modulation of PP1 to regulate differentially protein phosphorylation patterns in brain and gut. GBPI, its closest family member CPI (PKC-potentiated PP1 inhibitor) and two other family members, kinase-enhanced phosphatase inhibitor and phosphatase holoenzyme inhibitor, probably modulate integrated control of protein phosphorylation states in these and other tissues.

**Key words:** cell signalling, inhibitor, PKA (protein kinase A), PKC (protein kinase C), PP1 (protein phosphatase 1).

## INTRODUCTION

Protein phosphatases 1 and 2A (PP1 and PP2A) are prominent mammalian serine/threonine protein phosphatases. These phosphatases are major signal-transducing enzymes whose activities can be regulated by exogenous and endogenous agents [1–4]. Phosphatase regulation can contribute significantly to the modulation of key cellular processes including transcription, protein synthesis, metabolism, muscle contraction and cell division [5]. PP1 regulation can also alter information processing in neurons by regulating proteins that include neurotransmitter receptors, voltage-gated ion channels and ion pumps [3,6].

PP1 is regulated, and much of PP1 specificity is conferred, by a number of regulatory proteins that change PP1 activities when they are themselves phosphorylated and dephosphorylated by kinases and phosphatases [7], whose activities can be changed by altered cellular signals. For example, the phosphorylation state of the PP1 inhibitor DARPP-32 (dopamine- and cAMP-regulated phosphoprotein; molecular mass, 32 kDa) is increased by cocaine and amphetamine in striatum [8]. PKA (protein kinase A or cAMP-dependent protein kinase) phosphorylates the PP1 inhibi-

tors DARPP-32, Inhibitor-1 and NIPPI (nuclear inhibitor of PP1) [3,9]. PKG (protein kinase G or cGMP-dependent protein kinase) phosphorylates the PP1 inhibitor G-substrate [10]. Glycogen synthase kinase 3 phosphorylates the PP1 inhibitor Inhibitor-2 [11]. PKC phosphorylates CPI (PKC-potentiated PP1 inhibitor) [12], PHI (phosphatase holoenzyme inhibitor) [13] and KEPI (kinase-enhanced phosphatase inhibitor) [4]. Recently, integrin-linked kinase and Rho kinase phosphorylation of CPI have also been documented [14–16]. Phosphatases that terminate the activities of PP1-regulatory phosphoproteins [17] include PP2B (calcineurin), which dephosphorylates DARPP-32 and inactivates its PP1-inhibitory functions [18].

Phosphorylation and dephosphorylation events can dramatically change the ability of PP1 inhibitors to alter PP1 activities. PP1 inhibition increases 1000-fold owing to phosphorylation of DARPP-32, Inhibitor-1, G-substrate, CPI-17, PHI and KEPI [4,5,9,13,19]. In contrast, phosphorylation of NIPPI and Inhibitor-2 decreases their abilities to inhibit PP1 [11,20].

Thus, PP1 inhibitors are active cellular regulators that can alter patterns of cellular phosphorylation on the basis of signals received through broad classes of GPCRs (G-protein-coupled

Abbreviations used: PKA, protein kinase A; PKC, protein kinase C; DARPP, dopamine- and cAMP-regulated phosphoprotein; PP1, protein phosphatase 1; CPI, PKC-potentiated PP1 inhibitor; GBPI, gut and brain phosphatase inhibitor; GPCR, G-protein-coupled receptor; GST, glutathione S-transferase; KEPI, kinase-enhanced phosphatase inhibitor; NIPPI, nuclear inhibitor of PP1; ORF, open reading frame; PHI, phosphatase holoenzyme inhibitor; RT, reverse transcriptase; THOP, testis homologue of PHI; for brevity, the one-letter system for amino acids has been used: e.g. E28 is Glu<sup>28</sup>.

<sup>1</sup> To whom correspondence should be addressed (e-mail guhl@intra.nida.nih.gov).

The nucleotide sequence data reported have been submitted to the GenBank<sup>®</sup> Nucleotide Sequence Databases under the following accession numbers: human GBPI-1 cDNA, AY050671; mouse GBPI-1 cDNA, AF408400; mouse GBPI-2, AY179331; rat GBPI-1 cDNA, AY122322; human CPI cDNA, AY050670; mouse CPI cDNA, AY050672; rat CPI cDNA, AY050673; rat PHI-1 cDNA, AY122323; pig PHI-1 cDNA, AY122324; and *Drosophila melanogaster* KEPI cDNA, AY050669.

receptors) and other cell-surface receptors. Therefore PP1 inhibitors probably influence different functions in different cell types in which they are expressed. Protein phosphatase regulators could change cell-cycle parameters in dividing cells. They play many roles influencing mainly post-mitotic neurons in brain circuits, producing changes in neuronal processes [21].

We reported recently the cloning of a novel PKC-potentiated PP1 inhibitor, KEPI, which we identified by its up-regulation of mRNA in brains of morphine-treated rodents [4]. On the basis of the interesting profile of KEPI expression and regulation, characterizing the nature, roles and expression patterns of each of the protein phosphatase-regulatory phosphoproteins is of interest. We now describe GBPI (gut and brain phosphatase inhibitor), which has been identified by its similarity to KEPI sequences. We demonstrate that GBPI mRNAs are expressed in several brain regions as well as in gut. We identified an alternative transcript, GBPI-2, expressed in testis. We demonstrate that GBPI-1 is a potent and powerful inhibitor of PP1 enzymic activity when phosphorylated by PKC. Phospho-GBPI-1 enhances PP2A activity, although with lower potency. We show that inhibition of PP1 by PKC-phosphorylated GBPI-1 can be reversed by its subsequent phosphorylation by PKA. Each of these results demonstrates that GBPI is a new member of the interesting class of PP1-regulatory phosphoproteins and probably plays important roles at the junctions between PKC and PKA phosphoregulatory pathways in tissues such as brain, gut and testis.

## EXPERIMENTAL

### Production and purification of GBPI-1-fusion protein

Initial human and mouse cDNAs were identified to be human and mouse ESTs (expressed sequence tags) with sequence homologies to KEPI, including accession numbers AI767585 (GenBank®), 2382912 [IMAGE; A.T.C.C., Manassas, VA, U.S.A.], BG966186 (GenBank®) and 4984667 (IMAGE; Invitrogen, Carlsbad, CA, U.S.A.). cDNA sequences were confirmed by dideoxynucleotide sequencing. The 770 bp human cDNA, cloned in *EcoRI* and *NotI* sites of pT7T3D-Pac, contains an ORF (open reading frame) that includes a translation-initiation methionine and a stop codon. A translation-initiation site adapter with the sequence CCAATACTTCCATGgTGTCTTC (where 'g' represents a nucleotide replacement that provides a new *NcoI* restriction site) and a T3 primer were used to amplify a 0.7 kb segment of the cDNA. PCR products were digested with *NcoI* at the translation-initiation site and with *HindIII* at the polylinker site and cloned into *NcoI*–*HindIII* sites of the bacterial expression vector pET-30 (Novagen, Madison, WI, U.S.A.). The initiation methionine of pET30-GBPI-1 was positioned such that the ORF followed the His-tag peptide in-frame. Purification of the His–GBPI-1-fusion protein was performed as described previously [4]. The His–GBPI-1-fusion protein contains 44 amino acids of the His-tag peptide upstream of the N-terminal methionine residue of GBPI.

To produce the GST (glutathione S-transferase)–GBPI-1-fusion protein, an adapter with the sequence GACCAATGGATCC-ATGCTGTCTTC, which provided a new *BamHI* restriction site (underlined) 5' to the translation-initiation site of human GBPI-1, and a T3 primer were used to amplify a 0.7 kb fragment, using the human GBPI-1 cDNA plasmid as the template. The PCR fragment was digested with *BamHI* and *NotI* (at a polylinker site) and cloned into the *BamHI*–*NotI* site of the GST N-terminal fusion expression vector pGEX-4T-2 (Amersham Biosciences, Piscataway, NJ, U.S.A.) to form pGEX-GBPI-1. *Escherichia coli* BL21 were transformed with pGEX-GBPI-1, grown at 37 °C in

Lennox broth/ampicillin (50 µg/ml) to reach  $A_{600}$  0.7, induced with 0.2 mM isopropyl β-D-thiogalactoside and grown at 30 °C for 2 h. Expressing bacteria were lysed by sonication, the lysate was centrifuged at 10 000 g for 10 min at 4 °C and GST-tagged GBPI-1 protein was purified from the supernatant by affinity chromatography according to the manufacturer's instructions (GSTrap FF column; Amersham Biosciences). GST tag (224 amino acids) was removed from GBPI-1 protein by incubation with thrombin protease at 25 °C for 16 h. GBPI-1 protein was eluted from glutathione–Sepharose 4B columns, quantified by Bradford assays (Bio-Rad, Hercules, CA, U.S.A.) and checked for purity by SDS/PAGE (15 % gel). Purified recombinant GBPI-1 protein thus contained a glycine and a serine residue, N-terminal to the initiation methionine.

Full-length rat GBPI-1 cDNAs and human, mouse and rat cDNA clones for CPI and PHI were obtained by low-stringency screening of cDNA libraries, using the mouse GBPI-1 cDNA insert as a probe ([22], but also see [22a]) and by RT (reverse transcriptase)–PCR amplification using primers derived from EST alignments of cDNAs from rodent brain. *Drosophila melanogaster* KEPI (dKEPI) EST clones RE14405, RE18945, RE20685 and RE35817 were obtained from ResGen (Invitrogen) and inserted into *BamHI* and *XhoI* sites of the pFLC-1 vector. Shorter 1243 bp (RE14405 and RE20685) and longer 2344 bp (RE18945 and RE35817) transcripts were observed due to alternative polyadenylation of dKEPI mRNAs.

### RT-PCR to identify GBPI-1 transcripts in different tissues

Human cerebral cortical samples were obtained from rapidly frozen tissues obtained *post mortem*. Mouse brain and peripheral tissues were dissected after killing and immediately frozen in liquid nitrogen. Total RNA was extracted from brain tissues using RNazol B (Tel-Test, Friendswood, TX, U.S.A.). Single-strand cDNA was synthesized from total RNA using SuperScript™ first-strand synthesis system for RT–PCR (Gibco BRL, Rockville, MD, U.S.A.). Human MTC (multiple-tissue cDNA) panels MTC-I, including heart, brain, placenta, lung, liver, skeletal muscles, kidney and pancreas, and MTC-II, including spleen, thymus, prostate, testis, ovary, small intestine, colon and periphery blood leucocyte (Clontech, Palo Alto, CA, U.S.A.), served as templates to study human GBPI transcripts. Primer Express software (Applied Biosystems, Foster City, CA, U.S.A.) was used to design RT–PCR primers. hGBPI-5 (AGCTCCAGCGCTGGCTGGAGATGGAG) sense primer and hGBPI-3 (TCTGAGCCGGCTGAGTCTCCGGAG) antisense primer were used to amplify a 239 bp amplicon corresponding to human GBPI-1 mRNA. mGBPI-5 sense (GAGAAGAGAAGGAGGGCATCG) and mGBPI-3 antisense (TTTTTCAGCCAGTATCCAGGTCAG) primers were used to amplify a 437 bp amplicon corresponding to mouse GBPI-1 mRNA. mPHI-5 sense primer (CAAGGGAAGGTCACCGTCAAGTACG) and mPHI-3 antisense primer (TGGGGTGTGCTCAGCTTCTGCATGC) were used to amplify a 227 bp amplicon corresponding to mouse PHI mRNA. Two-step PCR programmes were used to amplify GBPI transcripts using brain region- and tissue-specific cDNAs as templates. Thermal cycling used a 95 °C, 8 min 'hot start', followed by seven cycles of 30 s at 94 °C and 2 min cycles that began at 72 °C but decreased in temperature by 1 °C for each cycle, followed by 45 cycles of 30 s at 94 °C, 2 min at 65 °C, followed by a final extension for 5 min at 65 °C. The amplified RT–PCR fragments corresponding to GBPI transcripts were analysed using 2 % agarose gels stained with ethidium bromide and 5 % acrylamide gels stained with SYBR® Green I (BioWhittaker Molecular Applications, Rockland, ME,

U.S.A.), using  $\Phi$ X174 RF DNA/*Hae*III fragments (Invitrogen) as molecular-mass standards. The amplicons were excised from agarose gels, purified using Concert™ PCR purification kits (Gibco BRL) and sequenced to confirm the sequence specificities of GBPI-1 amplification products.

### Sequence analyses and homology searches

cDNA sequences were assembled using Sequencher (version 3.0; Gene Codes Corp., Ann Arbor, MI, U.S.A.). BLAST searches (<http://www.ncbi.nlm.nih.gov/BLAST/>), Ensemble (<http://www.ensembl.org>) and Celera databases (<http://www.celera.com>) were used to map human and mouse genes. Relationships between the sequences of GBPI, CPI, PHI and KEPI were analysed using GCG GrowTree with Kimura protein distance correction methods (Genetics Computer Group, Madison, WI, U.S.A.). Potential phosphorylation sites were predicted with ExPASy Molecular Biology Server (<http://us.expasy.org>).

### Phosphorylation of recombinant GBPI-1 protein

Recombinant GBPI-1 protein was tested as a substrate for purified rat brain PKC (protein kinase C; Calbiochem, La Jolla, CA, U.S.A.) and bovine heart PKA catalytic subunit (Cell Signaling Technology, Beverly, MA, U.S.A.). PKC phosphorylation reactions were performed at 30 °C in 100  $\mu$ l of 20 mM Hepes (pH 7.4), 0.1 mM CaCl<sub>2</sub>, 10 mM MgCl<sub>2</sub>, 100  $\mu$ g/ml phosphatidylserine, 20  $\mu$ g/ml diacylglycerol, 100  $\mu$ M [ $\gamma$ -<sup>32</sup>P]ATP, 2 ng of PKC and 3  $\mu$ M His-GBPI-1 or GST-GBPI-1 protein. PKC-phosphorylated GBPI-1 was purified by PD-10 Sephadex column chromatography (Amersham Biosciences). PKC-phosphorylated GBPI was also used as PKA substrate in experiments in which PKA phosphorylations were performed at 30 °C in 100  $\mu$ l of 50 mM Tris/HCl (pH 7.4), 10 mM MgCl<sub>2</sub>, 200  $\mu$ M [ $\gamma$ -<sup>32</sup>P]ATP, 10 units of PKA and 3  $\mu$ M His-GBPI-1 or GST-GBPI-1 protein. For sequential phosphorylation studies, PKA- or PKC-phosphorylated GBPI-fusion proteins were purified, exchanged into appropriate buffers by PD-10 Sephadex column chromatography and then phosphorylated by PKC and PKA respectively. For time-course studies, reaction aliquots were sampled after 5, 10, 20, 30, 60, 90 and 120 min incubations. For kinetic studies, different concentrations of GBPI-1-fusion proteins were used as PKC and PKA substrates for 60 min. Phosphorylation was stopped by adding 1 ml of 25 % (w/v) trichloroacetic acid and 10  $\mu$ l of 1 mg/ml BSA at 4 °C. Phospho-GBPI-1 was precipitated by centrifugation at 10 000 g for 10 min at 4 °C and washed twice with 7.5 % trichloroacetic acid at 4 °C. <sup>32</sup>P-labelled proteins were assessed by scintillation counting and by SDS/PAGE followed by autoradiography. Triplicate data were analysed by non-linear regression using GraphPad (San Diego, CA, U.S.A.).

### Phosphopeptide mapping

His-GBPI-1, GST-GBPI-1 and GST-GBPI-M3-fusion proteins that were <sup>32</sup>P-labelled by incubation with PKC or PKA were separated by SDS/PAGE, stained with Coomassie Blue and detected by autoradiography. A radioactive band migrating with a mass of 30 kDa of His-GBPI or 52 kDa of GST-GBPI-1 was excised from the gel, washed overnight with 10 % (v/v) methanol and freeze-dried. Dried gel fragments were digested in 1 ml of trypsin solution (50  $\mu$ g/ml in 50 mM NH<sub>4</sub>HCO<sub>3</sub>, pH 8.0) at 37 °C overnight. The peptide solution was separated from the remain-

ing gel fragments, freeze-dried and dissolved in 10  $\mu$ l of electrophoresis solution (acetic acid/formic acid/water, 3:1:16, by vol.). Tryptic phosphopeptides were analysed by two-dimensional peptide mapping on cellulose TLC plates (Selecto Scientific, Suwanee, GA, U.S.A.) using electrophoresis as the first dimension and ascending chromatography in n-butanol/pyridine/acetic acid/water (13:10:2:8, by vol.) as a second dimension, as described in [23,24].

### Site-directed mutagenesis

Mutagenesis was performed using a two-step megaprimer PCR method [25] using the following oligonucleotides: M1, CCAG-ATGGGGAGAACCCATGTGAGGAGGTCCACTGGGCTTC; M2, CATGTAAGAAGGTCCACGCGGCTTCTGGGAGGA; and M3, GACCCAGCCGCTTGAAGTGAAGTATGACC (mutated nucleotides are shown in boldface). First-step PCR used the antisense primer GAGAGCTTCCAGGTCAATCTCA and human GBPI cDNA as templates. Second-step PCR used the sense oligonucleotide GGGGGATCCATGCTGTCTTCAA containing a *Bam*HI site, the megaprimer derived from the first-step PCR and the antisense primer from the first-step PCR to produce GBPI mutants. Second-step PCR products were digested with *Bam*HI at a site located in the vector pGEX-4T and with *Ssr*I at a site located in GBPI, and the resulting restriction fragment was shuttled into the wild-type pGEX-GBPI-1 at the same unique restriction sites. Sequences of the resulting mutant constructs pGEX-GBPI-M1 and pGEX-GBPI-M2 were confirmed by DNA sequencing. Mutant GST-GBPI-1-fusion proteins were expressed in *E. coli* BL21 and confirmed by SDS/PAGE.

### PP1 and PP2A assays

A protein phosphatase assay system (Gibco BRL) provided differential measurements of PP1 and PP2A activities in dephosphorylating the glycolytic enzyme phosphorylase *a*. Phosphorylase *a* was labelled with [ $\gamma$ -<sup>32</sup>P]ATP according to the manufacturer's instructions, purified by PD-10 Sephadex column chromatography (Amersham Biosciences) and [<sup>32</sup>P]phosphorylase *a* protein concentrations were measured by Bradford assays (Bio-Rad protein assay). Dephosphorylation reactions were performed with 0.3 unit of recombinant rabbit muscle PP1 $\alpha$  or 5 ng of bovine kidney PP2A<sub>1</sub> (Calbiochem) in 60  $\mu$ l volumes, containing 6  $\mu$ M [<sup>32</sup>P]phosphorylase and various concentrations of phospho-GBPI-1 or unphosphorylated GBPI-1 as inhibitors. Maximal phosphatase activities were assessed in reactions that used no inhibitors, and non-specific blank values were determined in reactions that contained no phosphatase. For peptide competition assays with potential PP1-binding amino acid sequences, decapeptide sequences were designed (see Figure 7) and synthesized (American Peptide Co., Vista, CA, U.S.A.) based on potential PP1-binding motifs of human GBPI (19–28), CPI (5–14), KEPI (17–26), and PHI-1 (24–33) [26]. We mixed 50  $\mu$ M of each decapeptide with 6  $\mu$ M [<sup>32</sup>P]phosphorylase *a* substrate and different concentrations of PKC-phosphorylated GBPI-1. Dephosphorylation reactions were initiated by the addition of 0.3 unit of recombinant rabbit muscle PP1 $\alpha$ . Samples were incubated at 30 °C for 20 min, proteins were precipitated with 160  $\mu$ l of 25 % trichloroacetic acid at 4 °C and centrifuged at 12 000 g for 5 min at 4 °C; free <sup>32</sup>P released into 200  $\mu$ l of supernatant aliquots was quantified by scintillation counting. Triplicate data were analysed by non-linear regression using GraphPad.

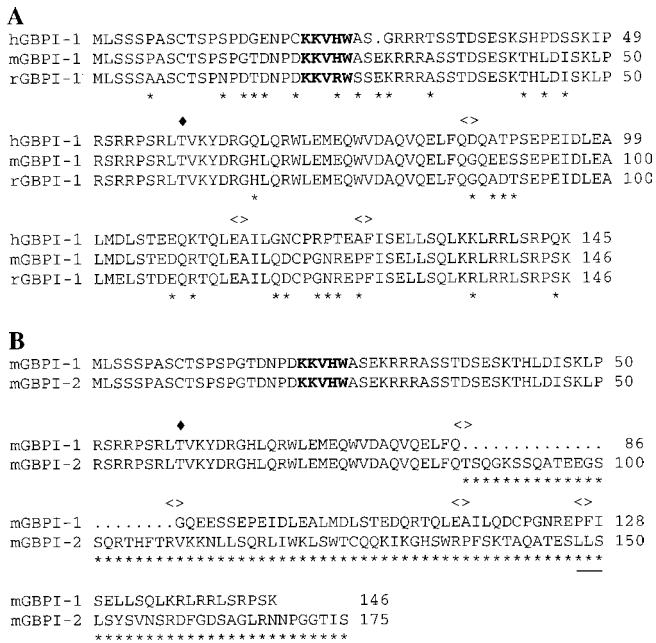


**Figure 1** Amino acid sequence alignments

(A) Human, mouse and rat GBPI-1 peptide sequences; (B) mouse GBPI-1 and -2 peptide sequences. '.', gap; \*, difference of amino acids; ◆, PKC phosphorylation site; <>, exon-intron junction. Potential PPI-binding consensus sequences are shown in boldface and potential transmembrane domain is underlined.

## RESULTS

### cDNA and amino acid sequences of GBPI

Protein-protein BLAST searches of GenBank® using KEPI amino acid sequences [4] as templates identified the hypothetical protein sequence FLJ20251 that displayed 42% identity with the 100 C-terminal residues of human KEPI. The FLJ20251 nucleotide sequences identified EST clones (A1767585/I.M.A.G.E. 2382912) that were obtained from A.T.C.C. The clones were found to contain the GBPI ORF and were used to synthesize fusion proteins. These sequences allowed definition of human, rat and mouse GBPI-1 cDNAs of 770, 760 and 740 bp respectively, each encoding complete coding sequences with initiation methionine and stop codons. In-frame stop codons were found in 5'-untranslated regions of cloned mouse, but not human or rat cDNAs.

Human and rodent GBPI-1s display approx. 80% nucleotide sequence and amino acid sequence identities. The 146-amino-acid rodent GBPI-1 sequence contains an additional glutamate (E28) not found in the 145-amino-acid human GBPI-1 sequence, decreasing its pI to 6.79 from the pI of 7.92 found in human GBPI-1. GCG plot structure predicts that GBPI-1 is a hydrophilic molecule with turns distributed regularly through its peptide sequence. The sequence contains four potential sites for phosphorylation by PKC and PKA and several sites for phosphorylation by casein kinase II. A consensus site for PKC phosphorylation (RLT<sup>58</sup>VK in human; Figure 1A) is similar to the PKC phosphorylation site (RVT<sup>38</sup>VK) identified for its close family member CPI. A consensus PPI-binding motif, with two basic amino acids followed by hydrophobic amino acids, is observed in the GBPI-1 N-terminal amino acids 21–25 (KKVHW). GBPI-1 lacks consensus sequences for signal peptides, transmembrane domains, myristoylation sites, glycosylation sites or coiled-coil structures.

### Tissue distribution of GBPI mRNA

Tissue-specific expression of GBPI was identified in human and mouse. A 239 bp human GBPI-1 amplicon was observed in amplification products from commercially prepared cDNAs from human colon, intestine and kidney mRNAs. Expression was most prominent in colon and intestine and in cDNAs prepared from mRNA extracted from post-mortem human cerebral cortical specimens (Figure 2A). No amplicons were noted in amplification products from commercially available human heart, liver, lung, pancreas, placenta, leucocyte, ovary, prostate, spleen, testis or thymus mRNA.

A 437 bp amplicon specific for mouse GBPI-1 was observed in mouse intestine, kidney, lung, spleen, stomach and brain. No significant mouse GBPI expression was noted in heart, liver or muscles. Studies of the regional expression of GBPI-1 expression in brain revealed highest levels of expression in cerebral cortex, hippocampus and midbrain (Figure 2B). In contrast, a 277 bp amplicon specific for mouse PHI was observed ubiquitously in cDNAs amplified from the same RNA extracted from all mouse tissues (results not shown).

Amplification of mRNA from mouse testis produced a 497 bp amplicon (Figure 2B). Sequence alignment of the testis-specific amplicon revealed a differentially spliced variant that contained an additional exon lying between exons 1 and 2 of the genomic sequences that encoded the GBPI-1 isoform. This additional mouse exon was flanked by consensus splice donor and acceptor sites in mouse genomic sequence. Interestingly, this additional exon yields both an additional amino acid sequence and a frameshift (Figure 1B). Thus, the resulting predicted 175-amino-acid translation product shares the 86 N-terminal amino acids with the isoform expressed in other tissues, but contains 89 novel amino acids at its C-terminus. We term the testis-specific protein 'GBPI-2'. GBPI-2 is larger and more basic (pI 10.94) than GBPI-1. GBPI-2 does retain a PPI consensus binding site (KKVHW) and a PKC phosphorylation site (RLTVK) in its N-terminal regions. GCG TransMem program predicts that GBPI-2 hydrophobic sequences near its C-terminal region SLLS-LSYSVNSRDFGDSAGL might form a transmembrane domain (Figure 1B, underlined). Such a topology would place the GBPI-2 N-terminal region intracellularly and its nine C-terminal amino acids extracellularly.

### Preparation and purification of GBPI-1-fusion protein

When the GBPI-1 cDNA was cloned in-frame with His-pET30 expression vector and induced in BL21 (DE3) or (DE3) pLysE *E. coli* cells with 1 mM isopropyl β-D-thiogalactoside for 1, 2, 3, 4 or 5 h, only very low amounts of intact fusion protein was expressed (results not shown). SDS/PAGE analyses of the His-GBPI-1-fusion proteins revealed evidence for substantial bacterial degradation. However, when human GBPI-1 cDNA was cloned into pGEX-4T-2, more intact GST-GBPI-1-fusion protein was obtained after GST-tag cleavage using thrombin protease and purification using glutathione-Sepharose 4B columns (Figure 3). This purified recombinant GBPI-1 displayed motility on SDS/polyacrylamide gels that corresponded to a mass of 28 kDa (Figure 3). The 30 kDa His-GBPI-1 species and GBPI-1 cleaved from GST-GBPI-1-fusion proteins displayed similar results in phosphorylation assays. Cleaved GBPI-1 and 30 kDa preparations of His-GBPI-1 each inhibited PPI enzymic activity 10-fold more potently than uncleaved GST-GBPI-1-fusion protein. The lower activities of the uncleaved GST-GBPI-1-fusion protein might conceivably explain its better expression in bacterial cells.

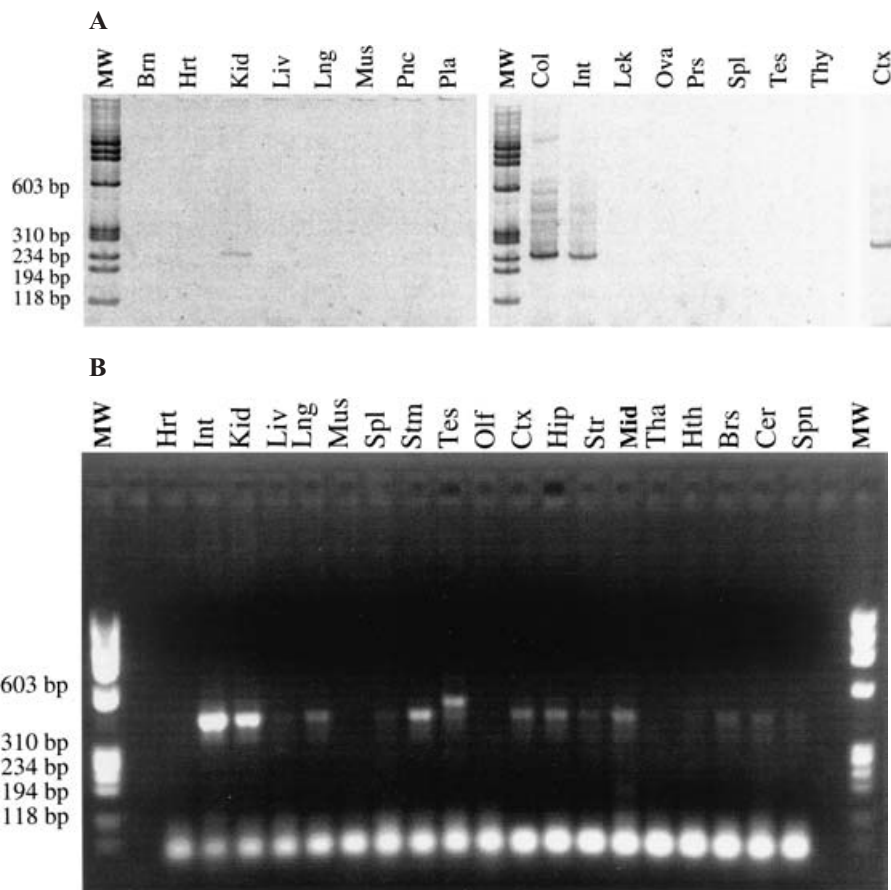


**Figure 2** Tissue distribution of PKC-potentiated PP1 inhibitor mRNAs

GBPI: RT-PCR of (A) human cDNA panel, and (B) mouse cDNA panel. Molecular-mass standards (MW) were  $\Phi$ X174/*Hae*III fragments. Hrt, heart; Kid, kidney; Liv, liver; Lng, lung; Mus, muscles; Pnc, pancreas; Pla, placenta; Col, colon; Int, intestine; Lek, leucocyte; Ova, ovary; Prs, prostate; Spl, spleen; Stm, stomach; Tes, testis; Thy, thymus; Brn, brain; Olf, olfactory bulb; Ctx, cortex; Hip, hippocampus; Str, striatum; Mid, mid brain; Tha, thalamus; Hth, hypothalamus; Brs, brain stem; Cer, cerebellum; Spn, spinal cord.

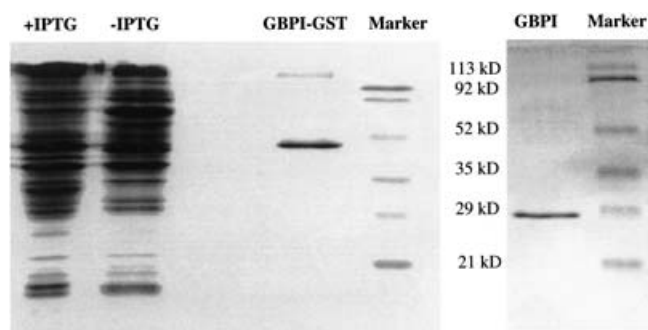


**Figure 3** Purification of GST-GBPI-1-fusion protein

Fusion protein was induced in the absence (–) or presence (+) of 0.2 mM isopropyl  $\beta$ -D-galactoside (IPTG). GBPI-GST, GST-GBPI-1 purified by affinity chromatography using a GST FF column. GBPI, cleavage product of the GBPI-1 fusion protein following the removal of the GST tag.

### PKC and PKA phosphorylation of the recombinant GBPI-1

Recombinant GBPI-1 protein can be phosphorylated by purified rat brain PKC preparations that contain mainly the conventional PKC isoforms  $\alpha$ ,  $\beta$ 1,  $\beta$ 2 and  $\gamma$ . Under these conditions, recombinant protein is phosphorylated with apparent  $K_m = 0.4 \pm$

$0.05 \mu\text{M}$ ,  $V_{\max} = 30.47 \pm 0.96 \text{ nmol} \cdot \text{mg}^{-1} \cdot \text{min}^{-1}$  and half-life ( $t_{1/2}$ ) =  $21.82 \pm 2.73 \text{ min}$  (Figure 4A, upper panel). At plateau time points, a near-stoichiometric ratio of phosphorylation,  $0.95 \pm 0.126 \text{ mol of P/mol of GBPI-1}$ , can be achieved. When the mobility of  $^{32}\text{P}$ -labelled GBPI-1 was analysed by SDS/PAGE and autoradiography (Figure 4A, middle panel), a dominant 30 kDa  $^{32}\text{P}$ -labelled band corresponding to GBPI-1 was observed. Phosphopeptide mapping demonstrates one predominantly tryptic,  $^{32}\text{P}$ -labelled peptide phosphorylated by PKC (Figure 4A, lower panel).

GBPI-1 could also be phosphorylated by the catalytic subunit of PKA, with results suggesting multiple potential PKA phosphorylation sites. After initial curve-fitting, we used two-phase exponential association and two-site hyperbolic models to analyse the time course and kinetics of PKA phosphorylation of GBPI-1.  $t_{1/2}$  values of  $1.71 \pm 0.29$  and  $42.75 \pm 4.54 \text{ min}$  (Figure 4B, upper panel) provided the best two-phase fit. Phosphorylation of recombinant GBPI-1 displayed  $K_{m1} = 4.77 \mu\text{M}$ ,  $K_{m2} = 34.36 \mu\text{M}$  and  $V_{\max} = 6.56 \text{ nmol} \cdot \text{mg}^{-1} \cdot \text{min}^{-1}$ . SDS/PAGE analyses of GBPI-1-fusion protein subjected to PKA phosphorylation displayed a  $^{32}\text{P}$ -labelled band with motility (Figure 4B, middle panel) similar to that displayed by GBPI-1-fusion proteins phosphorylated by PKC. Phosphopeptide mapping of PKA-pretreated GBPI-fusion protein revealed two  $^{32}\text{P}$ -labelled tryptic GBPI peptide fragments (Figure 4B, lower panel). Thus, both phosphopeptide mapping

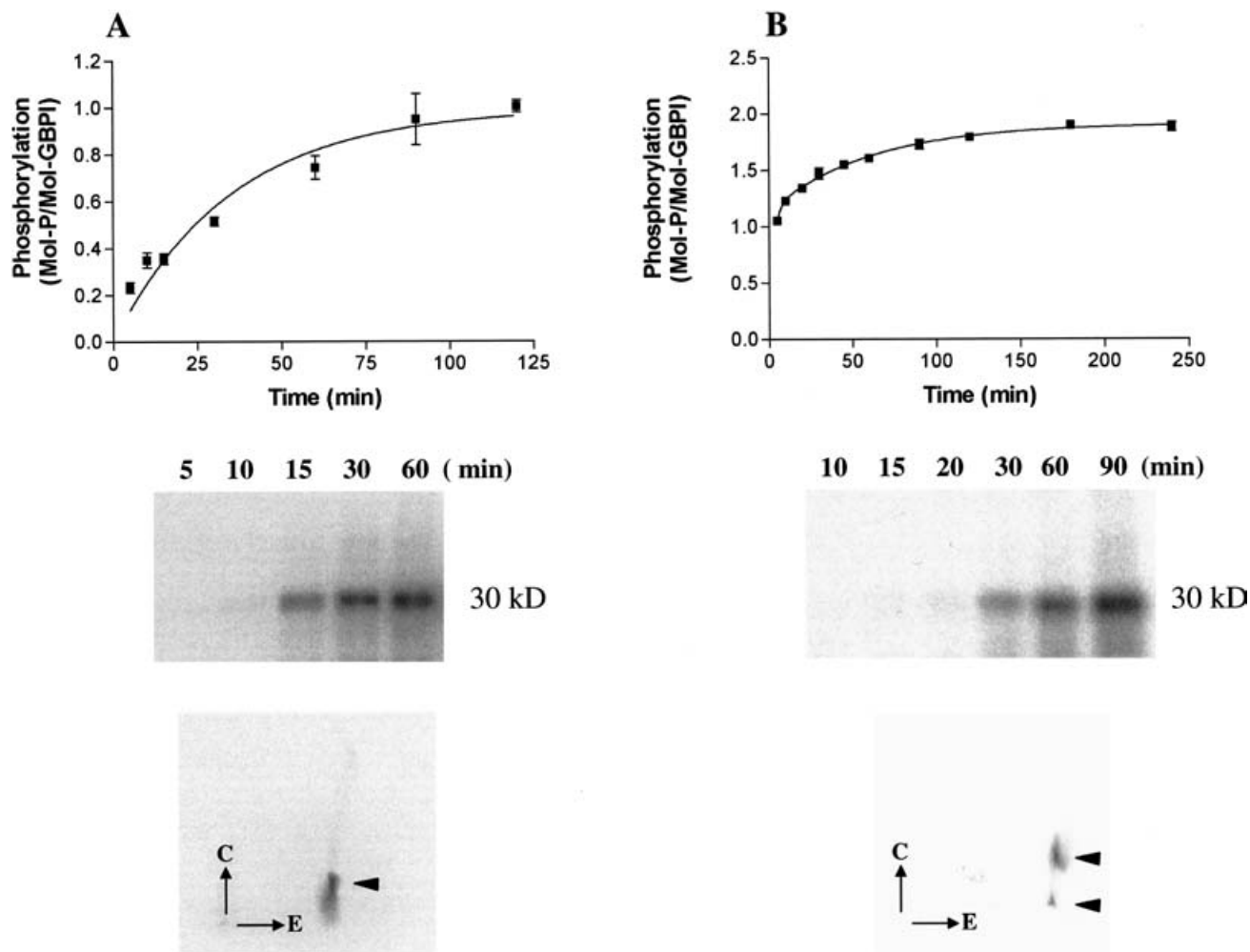


**Figure 4** PKC and PKA phosphorylation of GBPI-1

(A) Top: time-course kinetics of PKC phosphorylation of GBPI-1-fusion protein. (Middle) SDS/PAGE and autoradiography of  $^{32}\text{P}$ -labelled GBPI-1-fusion protein after various exposures to PKC. Bottom: autoradiogram of two-dimensional separations of PKC-phosphorylated GBPI-1-fusion protein tryptic phosphopeptides. 'E' represents the direction of electrophoresis and 'C' the direction of chromatography. Arrowheads point towards  $^{32}\text{P}$ -labelled phosphopeptides. (B) Top: time-course kinetics of PKA phosphorylation of GBPI-1-fusion protein. Middle: SDS/PAGE and autoradiography of GBPI-1-fusion protein labelled with  $^{32}\text{P}$  after various exposures to PKA. Bottom: autoradiogram of two-dimensional separations of PKA-phosphorylated GBPI-1-fusion protein tryptic phosphopeptides. Arrowheads point towards  $^{32}\text{P}$ -labelled phosphopeptides.

and kinetic data point towards the existence of at least two sites for the PKA phosphorylation of GBPI-1, although the sites could differ in their abilities to serve as PKA substrates.

When PKC- and PKA-phosphorylated GBPI-1 proteins were subsequently phosphorylated by PKA and PKC respectively, each displayed phosphorylation kinetics nearly identical with those displayed by GBPI-1 that had not been previously phosphorylated (results not shown). Each of these observations fails to support the existence of any substantial overlap between PKC and PKA phosphoacceptor sites on GBPI-1.

#### Inhibition of PP1 and activation of PP2A activity by PKC-phosphorylated GBPI-1

Phospho-GBPI-1 was produced by PKC preincubation of His-GBPI-1 or GBPI-1 cleaved from GST. Phospho-GBPI-1 inhibits the ability of recombinant rabbit muscle PP1 $\alpha$  to dephosphorylate  $^{32}\text{P}$ -labelled phosphorylase *a* with  $\text{IC}_{50} = 2.76 \pm 0.17$  nM (Figure 5A). PKC-phosphorylated GBPI-1 can also activate PP2A activity by more than 50% (Figure 5B) at high concentrations. Although PP2A activity can be stimulated up to 4-fold in the pre-

sence of 1 mM  $\text{Mn}^{2+}$ , the ability of PKC-phosphorylated GBPI-1 to activate PP2A is unchanged by 1 mM  $\text{Mn}^{2+}$  (results not shown). Neither non-phosphorylated GBPI-1 nor PKA-phosphorylated GBPI-1 was able to either inhibit PP1 or activate PP2A (Figures 5A and 5B). Interestingly, when PKC-phosphorylated GBPI-1 was further phosphorylated with PKA, the dually phosphorylated GBPI-1 lost its ability to inhibit PP1 (Figure 5A).

#### Site-directed mutagenesis at potential PP1-binding and PKC phosphorylation sites

Analyses of the activities of GST-GBPI-fusion protein mutants strengthened our confidence in several features conferred by specific features of this protein's sequence. Mutant M1 substituted two acidic glutamic residues for the two basic lysine residues at N-terminal positions 21 and 22 of GBPI-1. Thus, the potential PP1-binding site KKVHW was converted into EEVHW. Mutant M2 replaced the aromatic amino acid tryptophan with alanine to convert this site into KKVHA (Figure 6). Mutant M3 altered the PKC consensus phosphorylation site found at GBPI residues 56–60 (RLT58VK), replacing the phosphoacceptor threonine with

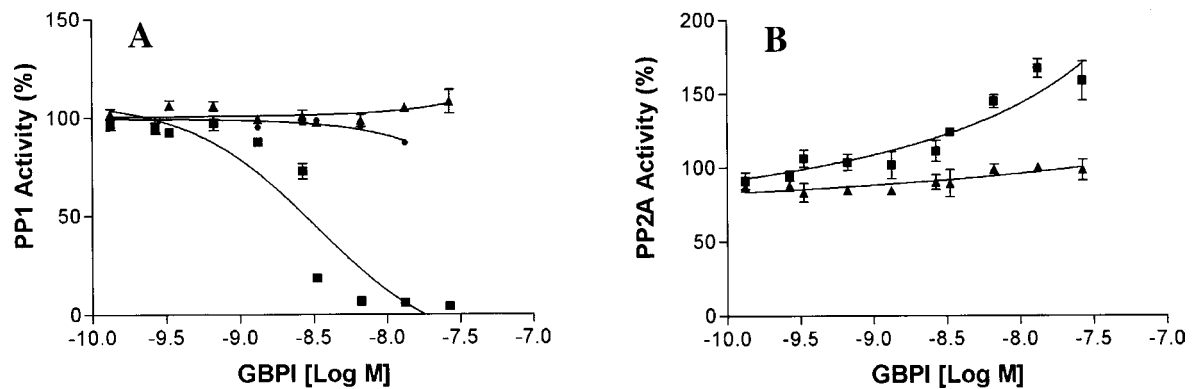


**Figure 5** Inhibition of PP1 and activation of PP2A by PKC-phosphorylated GBPI-1

(A) PP1 inhibition and (B) PP2A activation by PKC-phosphorylated GBPI-1.  $\blacktriangle$ , Unphosphorylated GBPI-1;  $\blacksquare$ , PKC-phosphorylated GBPI-1;  $\bullet$ , PKC- and PKA-dual-phosphorylated GBPI-1.

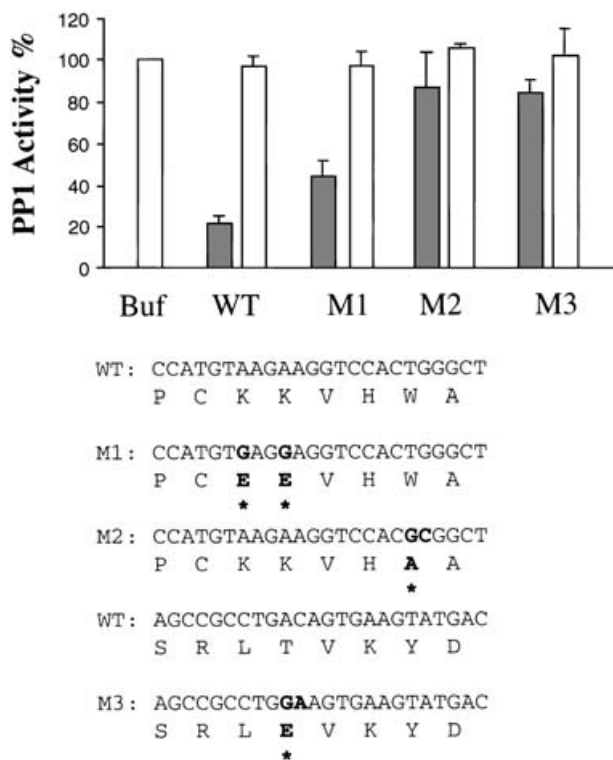


**Figure 6** Effects of site-directed mutagenesis on PP1 inhibition by wild-type and mutant GST-GBPIs

Mutated nucleotides are shown in boldface. Mutated amino acids are in boldface and marked with asterisks. Black bars, GST-GBPI-fusion proteins treated with PKC; open bars, non-phosphorylated GST-GBPI-fusion proteins.

glutamate (T58E) (Figure 6). Each of these mutations decreased the function of GBPI-1. PP1 enzymic activity was decreased by 100 nM concentrations of PKC-pretreated wild-type GST-GBPI-1-fusion protein to 21% of control values. However, mutants M1, M2 and M3 at the same concentration could only decrease this activity to 43, 87 and 84% of control values respectively (Figure 6). GST-GBPI-1 was a less potent PP1 inhibitor compared with His-GBPI-1.  $IC_{50}$  values were 20 nM for wild-type GBPI-fusion protein, but increased to 37, 448 and 2000 nM for M1, M2 and M3 respectively. Thus, substituting alanine for tryptophan

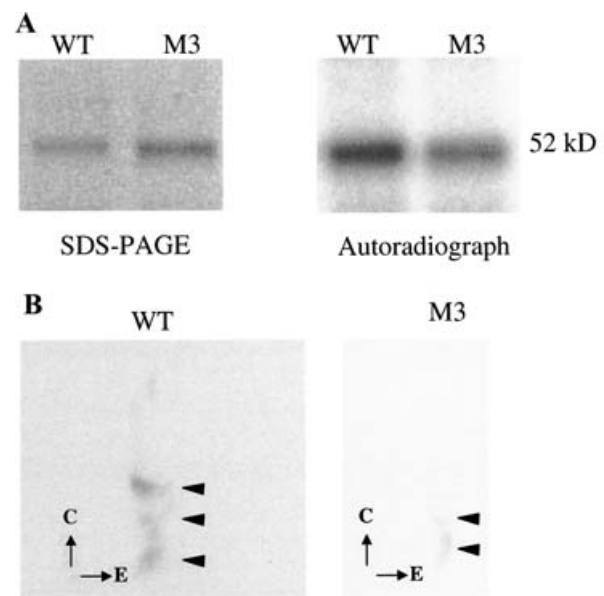
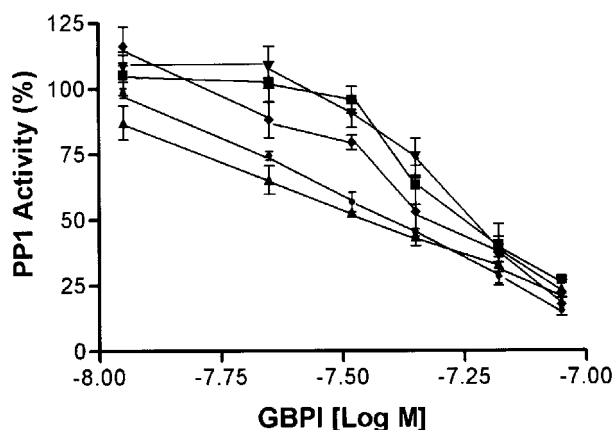


**Figure 7** Major PKC phosphorylation site of GBPI-1 responsible for PP1 inhibition

(A) SDS/PAGE and autoradiography of PKC-phosphorylated wild-type GST-GBPI-1 (WT) and mutant GST-GBPI-M3 (M3). (B) Phosphopeptide mapping of PKC-phosphorylated GST-GBPI-1 and GST-GBPI-M3. 'E' represents the direction of electrophoresis and 'C' the direction of chromatography. Arrowheads point towards  $^{32}P$ -labelled phosphopeptides.

produced greater loss of GBPI potency when compared with substituting acidic amino acids in place of basic amino acids at the canonical PP1-binding site. The threonine replacement at the phosphoacceptor site, T58E, produced dramatic losses of PP1-inhibitory activities, even though the glutamic residue substituted here produced the same sort of charge anticipated at this location in phosphorylated wild-type GBPI-1.

GST-GBPI-1 and GST-GBPI-M3-fusion proteins were treated with rat brain PKC subunits in the presence of  $[\gamma\text{-}^{32}P]\text{ATP}$  for 30 min at 30 °C and subjected to SDS/PAGE, autoradiography and phosphopeptide mapping. The T58E mutant GST-GBPI-M3-fusion protein displayed less PKC-mediated phosphorylation than wild-type GST-GBPI-1-fusion protein (Figure 7A), although the GST-GBPI-1-fusion tag itself contains consensus PKC phosphorylation motifs that provide additional



- GBPI (19-28) PCKKVVHWASG
- ▼ KEPI (17-26) GGARVFFQSP
- ◆ PHI-1 (24-33) PGPRVYFQSP
- ▲ CPI-17 (5-14) LGKRVLSKLQ
- GST-GBPI-1 Fusion Protein

**Figure 8** Decapeptide competition with PKC-phosphorylated GST-GBPI-1

Effects of decapeptides corresponding to GBPI (19–28) (■), KEPI (17–26) (▼), PHI-1 (24–33) (◆) and CPI (5–14) (▲) are shown. ●, Control experiments with no peptide competitors.

phosphorylated phosphopeptides (Figure 7B). The loss of the T58E phosphorylation site (Figure 7B) fits well with the loss of PKC-activated PP1-inhibitory activity of the mutant GST-GBPI-M3.

#### PP1 inhibition: competition between PKC-phosphorylated GBPI and potential PP1-binding peptides

We used 50  $\mu$ M concentrations of decapeptides, whose core sequences correspond to the PP1 consensus binding sites (R/KVXF/W) of human GBPI (residues 19–28), CPI (residues 5–14), KEPI (residues 17–26) and PHI-1 (residues 24–33) to compete for the PP1-inhibitory activity of PKC-phosphorylated GST-GBPI-1 fusion protein. GBPI (19–28), KEPI (17–26) and PHI-1 (24–33) decapeptides could each almost completely block inhibition of PP1 by PKC-phosphorylated GST-GBPI-1, although the decapeptide corresponding to CPI (5–14) had no effect (Figure 8). The CPI (5–14) core sequence of decapeptide (RVLS) does differ from PP1-binding consensus sequences (R/KVXF/W).

The inhibition displayed by GBPI (19–28), KEPI (17–26) and PHI-1 (24–33) decapeptides displays competitive features. Whereas 50  $\mu$ M concentrations of these three decapeptides could produce these effects when PKC-phosphorylated GST-GBPI-1 concentrations were less than 30 nM, no decapeptide could effectively compete with 90 nM concentrations of PKC-phosphorylated GBPI-1 (Figure 8). Studies at 30 nM concentrations of PKC-phosphorylated GST-GBPI-1 suggested the rank order of efficacy as follows: KEPI (17–26) > GBPI (19–28) > PHI-1 (24–33) > CPI (5–14). Thus, 50  $\mu$ M KEPI (17–26) or GBPI (19–28) or PHI-1 (24–33) decapeptide appeared to increase  $IC_{50}$  values for PKC-phosphorylated GST-GBPI-1 2–3-fold.

#### DISCUSSION

The present study functionally identifies a novel member of the PKC-potentiated PP1 inhibitor family that we term GBPI. We discuss this work in relationship to the comparative patterns of GBPI mRNA expression, structure–function relationships of GBPI and examples of the ways in which GBPI expression might alter the properties of expressing cell types and tissues and provide a novel drug target. The present study defines a molecule that can act at important modulatory junctions between PKC and PKA pathways in gut, brain and testis.

GBPI is now one of four PKC-potentiated PP1 inhibitors that have been functionally identified in humans and mice: GBPI, CPI, KEPI and PHI. There is only a single apparent *D. melanogaster* PP1 inhibitor family member, namely dKEPI. Neither *Caenorhabditis elegans* nor *Saccharomyces cerevisiae* has a clear homologue [27–29]. Unique patterns of tissue- and brain-region expressions also distinguish these transcripts. PHI is ubiquitously expressed. GBPI, CPI and KEPI are each differentially expressed in different tissues, different cell types and even different subcellular regions. GBPI-1 is prominently expressed in gastrointestinal tissues and moderately expressed in several brain regions. GBPI and CPI mRNAs are rare in skeletal muscles, but abundant in gastrointestinal or aortic smooth-muscle tissues [19]. KEPI is highly expressed in heart and skeletal muscles, but not in gastrointestinal tissues.

This family may have another member. Mouse EST sequences AV267143, AV280527, AV278668, AV204981, AV268589, AV040646, AV046230, AI429188, AK005938, AI595538, AA062392 and AK016819 align closely with the mouse 1A4 locus whose sequences provide the closest fit to PHI. Since each of these ESTs derives from testis, we tentatively name this new potential family member ‘testis homologue of PHI’ or ‘THOP’. Genomic THOP sequences found in the contig NW000166 display a single exon whose ORF encodes an apparent THOP protein that retains its PP1-binding motif ‘RVYF’, but lacks the consensus PKC phosphorylation site found in each of the other family members. Taken together, the present results suggest that GBPI is thus a member of a family of perhaps seven related sequences encoded by at least five distinct genes (Figure 9).

The structure–function results from the present mutagenesis studies may provide insights into the molecular basis for these physiological observations. Many proteins that interact with PP1 contain a canonical PP1-binding sequence (R/KVXF/W) [7,26]. The potential PP1-binding site (<sup>21</sup>KKVHW<sup>25</sup>) of GBPI is similar to that found in the PKA-potentiated PP1 inhibitor DARPP-32 (<sup>7</sup>KKIQF<sup>11</sup>), which has also been characterized by phosphopeptide inhibition and mutagenesis studies [30,31]. Double mutations of K21E – K22E in GBPI-1 increased  $IC_{50}$  only 2-fold, suggesting that the basic amino acids in the R/KVXF/W sequence might be less important than aromatic residues (Figure 6). These observations are similar to those observed in DARPP-32. Phosphopeptides that mimic the PP1 recognition motif of DARPP-32 and PKA phosphorylation site are equipotent with or without a basic amino acid at its KKIQF site [32], K7E mutation increases  $IC_{50}$  only 4-fold and K8E mutation decreases  $IC_{50}$  1.5-fold [30]. Peptide modelling (CGC PepPlot) predicts that the GBPI R/KVXF/W motif forms an amphipathic  $\beta$ -sheet that might interact with the interface of the two PP1  $\beta$ -sheets, which form a ‘ $\beta$ -sandwich’ in the PP1 crystal structure [33,34]. Thus, interactions between GBPI  $\beta$ -sheet and PP1  $\beta$ -sandwich provide a plausible interaction that could well modulate the activities of the PP1 phosphatase active site, which is located opposite to the  $\beta$ -sandwich in PP1 crystal structures [35]. Interestingly, substituting glutamic residues for lysine residues 21



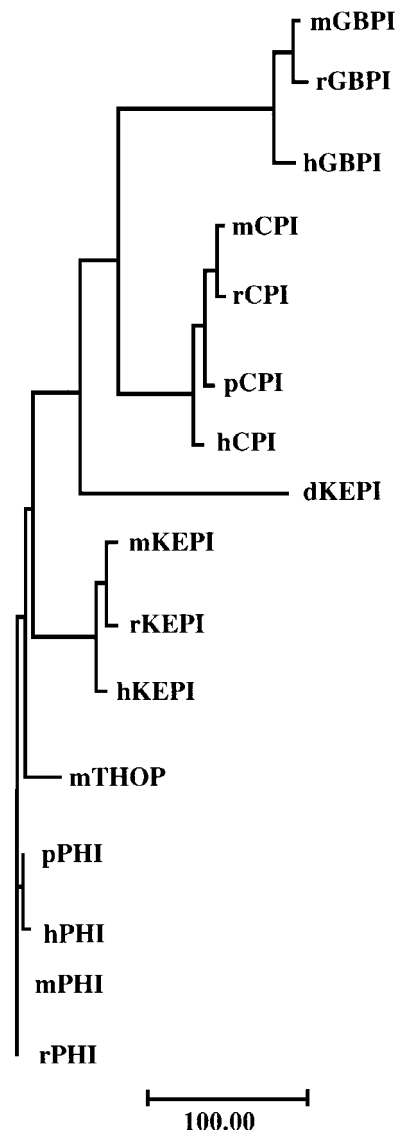


**Figure 9** Phylogram for PKC-potentiated PP1-inhibitory proteins

The scale bar represents the estimated number of substitutions per 100 amino acids. The branch lengths are proportional to evolution distances (CGC GrowTree).

and 22 in the putative PP1-regulatory/binding site of GBPI does not appear to alter the molecule's PepPlot  $\beta$ -sheet conformation score, whereas the W25A mutant eliminates  $\beta$ -sheet conformation scores for these sequences.

Results from mutagenesis studies and phosphopeptide mapping provide molecular characterization of GBPI phosphoregulation. Substitution of the consensus PKC phosphoacceptor site threonine with glutamate in the mutant T58E inactivates GBPI-1, as it does with mutagenesis of the corresponding residue in CPI (T38E) [36]. Phosphopeptide mapping of His-GBPI-1, GST-GBPI-1 and GST-GBPI-M3 appears to confirm that T58 is the primary PKC phosphorylation site and is thus probably responsible for the PKC actions in activating the ability of GBPI-1 to inhibit PP1. Further, this phosphopeptide is eliminated in the T58E GST-GBPI-M3 mutant, leaving only background phosphorylation of the GST-fusion tag. A weaker phosphopeptide spot representing a highly mobile peptide migrating near the top of the PKC phospho-

peptide maps could relate to an additional PKC phosphorylation site, as noted for CPI [37]. Phosphorylation of this second CPI site required prior phosphorylation of the residue (T38) homologous with T58 of GBPI, and appeared to be not related to PKC activation [15].

The subsequent PKA activity could reverse the physiological effects of prior PKC activation of GBPI. However, several lines of evidence indicate that the two kinases were not acting at the same site. (1) The consensus PKA sites [R/K(2)XS/T] in GBPI-1, namely T32, S33, S55 and S141, are different from the consensus PKC sites (S/TXR/K), S27, S45, S51 and T58. (2) PKA phosphorylation kinetics was virtually identical whether the His-GBPI-1 substrate used had been previously phosphorylated by PKC or not. (3) PKC phosphorylation kinetics was virtually identical whether the His-GBPI-1 substrate used had been previously phosphorylated by PKA or not. (4) PKA conferred similar patterns of phosphorylation on wild-type GST-GBPI-1 and the T58E mutant GST-GBPI-M3 in which the PKC phosphoacceptor site was eliminated (results not shown). (5) Initial mass spectrographic peptide 'fingerprint' studies identify one of the PKA sites, consistent with phosphorylation of T32, separate from the T58 site for PKC phosphorylation, indicated by phosphopeptide mapping, to lie on a separate tryptic fragment (A.S. Woods, Q.-R. Liu and G.R. Uhl, unpublished work). In contrast, it is quite plausible that nearby interactions could be responsible for the interactive effects of PKC- and PKA-mediated phosphorylations. PKA phosphorylation of the GBPI residue T32 could influence PKC-activated GBPI-1-inhibitory activity by interference with PP1 binding, owing to the proximity of T32 to the crucial PP1-binding residue W25. PKA phosphorylation of the GBPI residue S55 could even influence PKC-activated GBPI-1-inhibitory activity by interference with the sites for PKC activation, since S55 is close to T58.

Interactions between different phosphatase inhibitors and different phosphatases display complexities as well as similarities. PP1-regulatory binding sites probably differ from inhibitor to inhibitor in ways that involve more than primary amino acid sequences. The consequences of inhibitor-phosphatase interaction could also differ from phosphatase-interacting target protein to phosphatase-interacting inhibitory protein, and from phosphatase to phosphatase. Whereas many proteins that do not bind to PP1 display the R/KVXF/W motif [26], the potent PKC-potentiated PP1 inhibitor CPI does not contain an R/KVXF/W motif. Deletion experiments in which 34 N-terminal amino acids of CPI were deleted and PP1-inhibitory potencies retained do fit [36] with our peptide competition data in which CPI 5-14 sequences including the 8-KRVLS-12 motif are ineffective in competing for PP1 inhibition of GBPI-1. Another level of complexity appears to derive from the different patterns of functional interaction between different inhibitors and different phosphatases that appear to be revealed by peptide competition studies. Similar decapeptide competition experiments that display approx. 30 nM potency of GBPI-fusion protein in overcoming PP1 inhibition caused by 50  $\mu$ M competing peptide reveal approx. 3 nM apparent potencies of NIPPI in similar assays [26]. Differences between the phosphatase subunits and/or influences of additional subunits underline recently reported differences in inhibition of myosin phosphatase holoenzyme. The PKC-potentiated PP1 inhibitors CPI, PHI-1 and KEPI are reported to be potent inhibitors of myosin phosphatase holoenzyme [13,15,19]. In contrast, the PKA-potentiated PP1 inhibitors DARPP-32 and Inhibitor-1 are ineffective [38].

GBPI and its family members are thus well positioned biochemically to play a significant role in integrating PKC and PKA signals and plausibly signals from other cellular signalling

cascades. In initial experiments, we have identified apparent phosphorylation on one or more of the multiple consensus casein kinase II phosphorylation sites identified in GBPI's sequence (results not shown). Integrin-linked kinase, calmodulin kinase II, Rho kinase, p21-activated kinase, PKG and PKN (protein kinase N) have also been shown to phosphorylate and possibly regulate GBPI family members [14–16,37,39,40]. Nevertheless, it is a specific activity of GBPI to allow simultaneous or even subsequent PKA activation to negate the effects of PKC activation that has drawn our attention, and has not been clearly documented to our knowledge. GBPI could provide a locus for physiological integration between ligands that differentially activate the GTP-binding protein  $G_s$  and those that couple with  $G_{i/o/q}$ -coupled receptors. Signal-transducing roles of GBPI, KEPI and other family members are probably controlled in a temporal and spatial manner by post-translational modification, protein scaffold binding, transcription regulation, kinase/phosphatase activities and/or by extracellular signals. Nevertheless, PKC activation by calcium, inositol (1,4,5)-trisphosphate and diacylglycerol probably activate GBPI and lead to PP1 inhibition in many circumstances. Inactivated PP1 could fail to dephosphorylate substrates that could include neurotransmitter transporters, GPCRs and cAMP-response-element-binding proteins. Active GBPI would shift the equilibrium in favour of longer phosphorylation half-lives and alter cellular effects that probably include desensitization of GPCRs, reductions in neurotransmitter reuptake and stimulation of transcription at promoters such as those that contain important phosphorylation-sensitive cAMP-response elements.

The present results provide targets for specific physiological regulatory mechanisms that could be controlled in a tissue-specific and subcellular-compartment-specific fashion. In addition, they provide targets for pharmaceutical developments. Okadaic acid and most other currently available drugs that inhibit broadly expressed PP1 and PP2A can exhibit substantial toxicities [41]. Many clinically useful drugs act at important but less widespread targets, such as serine/threonine phosphatase PP2B [42]. Conceivably, drugs that could alter PP1 and/or PP2A modulation by the less ubiquitous phosphoproteins in the GBPI/KEPI gene family could provide interesting novel therapeutics for disorders of brain, gut, muscles and testis.

This work was financially supported by NIDA-IRP (NIH, DHSS). We acknowledge helpful discussions with Tsung-Ping Su (Cellular Neurobiology Research Branch, NIDA/NIH, Baltimore, MD, U.S.A.) and Pui-Kwong Chan (Department of Pharmacology, Baylor College of Medicine, Houston, TX, U.S.A.). Some of the gene alignments were generated using the Celera Discovery System and Celera genomics-associated databases.

## REFERENCES

- Sontag, E. (2001) Protein phosphatase 2A: the Trojan Horse of cellular signaling. *Cell Signal*, **13**, 7–16
- Cohen, P. T. (2002) Protein phosphatase 1 – targeted in many directions. *J. Cell Sci.* **115**, 241–256
- Greengard, P., Allen, P. B. and Nairn, A. C. (1999) Beyond the dopamine receptor: the DARPP-32/protein phosphatase-1 cascade. *Neuron* **23**, 435–447
- Liu, Q. R., Zhang, P. W., Zhen, Q., Walthers, D., Wang, X. B. and Uhl, G. R. (2002) KEPI, a PKC-dependent protein phosphatase 1 inhibitor regulated by morphine. *J. Biol. Chem.* **277**, 13312–13320
- Cohen, P. (1989) The structure and regulation of protein phosphatases. *Annu. Rev. Biochem.* **58**, 453–508
- Fienberg, A. A., Hiroi, N., Mermelstein, P. G., Song, W., Snyder, G. L., Nishi, A., Cheramy, A., O'Callaghan, J. P., Miller, D. B., Cole, D. G. et al. (1998) DARPP-32: regulator of the efficacy of dopaminergic neurotransmission. *Science* **281**, 838–842
- Aggen, J. B., Nairn, A. C. and Chamberlin, R. (2000) Regulation of protein phosphatase-1. *Chem. Biol.* **7**, R13–R23
- Svenningsson, P., Lindskog, M., Ledent, C., Parmentier, M., Greengard, P., Fredholm, B. B. and Fisone, G. (2000) Regulation of the phosphorylation of the dopamine- and cAMP-regulated phosphoprotein of 32 kDa *in vivo* by dopamine D1, dopamine D2, and adenosine A2A receptors. *Proc. Natl. Acad. Sci. U.S.A.* **97**, 1856–1860
- Bollen, M. and Stalmans, W. (1992) The structure, role, and regulation of type 1 protein phosphatases. *Crit. Rev. Biochem. Mol. Biol.* **27**, 227–281
- Hall, K. U., Collins, S. P., Gamm, D. M., Massa, E., DePaoli-Roach, A. A. and Uhler, M. D. (1999) Phosphorylation-dependent inhibition of protein phosphatase-1 by G-substrate. A Purkinje cell substrate of the cyclic GMP-dependent protein kinase. *J. Biol. Chem.* **274**, 3485–3495
- Park, I. K., Roach, P., Bondor, J., Fox, S. P. and DePaoli-Roach, A. A. (1994) Molecular mechanism of the synergistic phosphorylation of phosphatase inhibitor-2. Cloning, expression, and site-directed mutagenesis of inhibitor-2. *J. Biol. Chem.* **269**, 944–954
- Li, L., Eto, M., Lee, M. R., Morita, F., Yazawa, M. and Kitazawa, T. (1998) Possible involvement of the novel CPI-17 protein in protein kinase C signal transduction of rabbit arterial smooth muscle. *J. Physiol. (Cambridge, U.K.)* **508**, 871–881
- Eto, M., Karginov, A. and Brautigan, D. L. (1999) A novel phosphoprotein inhibitor of protein type-1 phosphatase holoenzymes. *Biochemistry* **38**, 16952–16957
- Deng, J. T., Sutherland, C., Brautigan, D. L., Eto, M. and Walsh, M. P. (2002) Phosphorylation of the myosin phosphatase inhibitors, CPI-17 and PHI-1, by integrin-linked kinase. *Biochem. J.* **367**, 517–524
- Erdodi, F., Kiss, E., Walsh, M. P., Stefansson, B., Deng, J. T., Eto, M., Brautigan, D. L. and Hartshorne, D. J. (2003) Phosphorylation of protein phosphatase type-1 inhibitory proteins by integrin-linked kinase and cyclic nucleotide-dependent protein kinases. *Biochem. Biophys. Res. Commun.* **306**, 382–387
- Koyama, M., Ito, M., Feng, J., Seko, T., Shiraki, K., Takase, K., Hartshorne, D. J. and Nakano, T. (2000) Phosphorylation of CPI-17, an inhibitory phosphoprotein of smooth muscle myosin phosphatase, by Rho-kinase. *FEBS Lett.* **475**, 197–200
- Mulkey, R. M., Endo, S., Shenolikar, S. and Malenka, R. C. (1994) Involvement of a calcineurin/inhibitor-1 phosphatase cascade in hippocampal long-term depression. *Nature (London)* **369**, 486–488
- Nishi, A., Snyder, G. L., Nairn, A. C. and Greengard, P. (1999) Role of calcineurin and protein phosphatase-2A in the regulation of DARPP-32 dephosphorylation in neostriatal neurons. *J. Neurochem.* **72**, 2015–2021
- Eto, M., Ohmori, T., Suzuki, M., Furuya, K. and Morita, F. (1995) A novel protein phosphatase-1 inhibitory protein potentiated by protein kinase C. Isolation from porcine aorta media and characterization. *J. Biochem. (Tokyo)* **118**, 1104–1107
- Beullens, M., Van Eynde, A., Bollen, M. and Stalmans, W. (1993) Inactivation of nuclear inhibitory polypeptides of protein phosphatase-1 (NIPP-1) by protein kinase A. *J. Biol. Chem.* **268**, 13172–13177
- Mills, J., Digiacylioglu, M., Legg, A. T., Young, C. E., Young, S. S., Barr, A. M., Fletcher, L., O'Connor, T. P. and Dedhar, S. (2003) Role of integrin-linked kinase in nerve growth factor-stimulated neurite outgrowth. *J. Neurosci.* **23**, 1638–1648
- Liu, Q. R., Lopez-Corcuera, B., Mandiyan, S., Nelson, H. and Nelson, N. (1993) Molecular characterization of four pharmacologically distinct  $\gamma$ -aminobutyric acid transporters in mouse brain. *J. Biol. Chem.* **268**, 2106–2112
- Liu, Q. R., Lopez-Corcuera, B., Mandiyan, S., Nelson, H. and Nelson, N. (1993) Erratum. *J. Biol. Chem.* **268**, 9156
- Liu, Q. R. and Chan, P. K. (1991) Formation of nucleophosmin/B23 oligomers requires both the amino- and the carboxyl-terminal domains of the protein. *Eur. J. Biochem.* **200**, 715–721
- Chan, P. K., Liu, Q. R. and Durban, E. (1990) The major phosphorylation site of nucleophosmin (B23) is phosphorylated by a nuclear kinase II. *Biochem. J.* **270**, 549–552
- Sarkar, G. and Sommer, S. S. (1990) The 'megaprimer' method of site-directed mutagenesis. *Biotechniques* **8**, 404–407
- Wakula, P., Beullens, M., Ceulemans, H., Stalmans, W. and Bollen, M. (2003) Degeneracy and function of the ubiquitous RVXF motif that mediates binding to protein phosphatase-1. *J. Biol. Chem.* **278**, 18817–18823
- Kennelly, P. J., Oxenrider, K. A., Leng, J., Cantwell, J. S. and Zhao, N. (1993) Identification of a serine/threonine-specific protein phosphatase from the archaeobacterium *Sulfolobus solfataricus*. *J. Biol. Chem.* **268**, 6505–6510
- Tu, J. and Carlson, M. (1994) The GLC7 type 1 protein phosphatase is required for glucose repression in *Saccharomyces cerevisiae*. *Mol. Cell. Biol.* **14**, 6789–6796
- Feng, Z. H., Wilson, S. E., Peng, Z. Y., Schlender, K. K., Reimann, E. M. and Trumbly, R. J. (1991) The yeast GLC7 gene required for glycogen accumulation encodes a type 1 protein phosphatase. *J. Biol. Chem.* **266**, 23796–23801
- Huang, H. B., Horiuchi, A., Watanabe, T., Shih, S. R., Tsay, H. J., Li, H. C., Greengard, P. and Nairn, A. C. (1999) Characterization of the inhibition of protein phosphatase-1 by DARPP-32 and inhibitor-2. *J. Biol. Chem.* **274**, 7870–7878

- 31 Kwon, Y. G., Huang, H. B., Desdouits, F., Girault, J. A., Greengard, P. and Nairn, A. C. (1997) Characterization of the interaction between DARPP-32 and protein phosphatase 1 (PP-1): DARPP-32 peptides antagonize the interaction of PP-1 with binding proteins. *Proc. Natl. Acad. Sci. U.S.A.* **94**, 3536–3541
- 32 Hemmings, Jr, H. C., Nairn, A. C., Elliott, J. I. and Greengard, P. (1990) Synthetic peptide analogs of DARPP-32 (*M*, 32,000 dopamine- and cAMP-regulated phosphoprotein), an inhibitor of protein phosphatase-1. Phosphorylation, dephosphorylation, and inhibitory activity. *J. Biol. Chem.* **265**, 20369–20376
- 33 Maynes, J. T., Bateman, K. S., Cherney, M. M., Das, A. K., Luu, H. A., Holmes, C. F. and James, M. N. (2001) Crystal structure of the tumor-promoter okadaic acid bound to protein phosphatase-1. *J. Biol. Chem.* **276**, 44078–44082
- 34 Eglhoff, M. P., Johnson, D. F., Moorhead, G., Cohen, P. T., Cohen, P. and Barford, D. (1997) Structural basis for the recognition of regulatory subunits by the catalytic subunit of protein phosphatase 1. *EMBO J.* **16**, 1876–1887
- 35 Eglhoff, M. P., Cohen, P. T., Reinemer, P. and Barford, D. (1995) Crystal structure of the catalytic subunit of human protein phosphatase 1 and its complex with tungstate. *J. Mol. Biol.* **254**, 942–959
- 36 Hayashi, Y., Senba, S., Yazawa, M., Brautigam, D. L. and Eto, M. (2001) Defining the structural determinants and a potential mechanism for inhibition of myosin phosphatase by the protein kinase C-potentiated inhibitor protein of 17 kDa. *J. Biol. Chem.* **276**, 39858–39863
- 37 Dubois, T., Howell, S., Zemlickova, E., Learmonth, M., Cronshaw, A. and Aitken, A. (2003) Novel *in vitro* and *in vivo* phosphorylation sites on protein phosphatase 1 inhibitor CPI-17. *Biochem. Biophys. Res. Commun.* **302**, 186–192
- 38 Alessi, D., MacDougall, L. K., Sola, M. M., Ikebe, M. and Cohen, P. (1992) The control of protein phosphatase-1 by targeting subunits. The major myosin phosphatase in avian smooth muscle is a novel form of protein phosphatase-1. *Eur. J. Biochem.* **210**, 1023–1035
- 39 Hamaguchi, T., Ito, M., Feng, J., Seko, T., Koyama, M., Machida, H., Takase, K., Amano, M., Kaibuchi, K., Hartshorne, D. J. et al. (2000) Phosphorylation of CPI-17, an inhibitor of myosin phosphatase, by protein kinase N. *Biochem. Biophys. Res. Commun.* **274**, 825–830
- 40 Takizawa, N., Koga, Y. and Ikebe, M. (2002) Phosphorylation of CPI17 and myosin binding subunit of type 1 protein phosphatase by p21-activated kinase. *Biochem. Biophys. Res. Commun.* **297**, 773–778
- 41 Sheppeck, II, J. E., Gauss, C. M. and Chamberlin, A. R. (1997) Inhibition of the Ser-Thr phosphatases PP1 and PP2A by naturally occurring toxins. *Bioorg. Med. Chem.* **5**, 1739–1750
- 42 Liu, J., Farmer, Jr, J. D., Lane, W. S., Friedman, J., Weissman, I. and Schreiber, S. L. (1991) Calcineurin is a common target of cyclophilin–cyclosporin A and FKBP–FK506 complexes. *Cell (Cambridge, Mass.)* **66**, 807–815

Received 15 January 2003/10 September 2003; accepted 16 September 2003  
Published as BJ Immediate Publication 16 September 2003, DOI 10.1042/BJ20030128